Atomization energies of the carbon clusters C $_n$ (n = 2-10) revisited by means of W4 theory as well as density functional, Gn, and CBS methods

Amir Karton [a]; Alex Tarnopolsky [a]; Jan M.L. Martin [a]

[a] Department of Organic Chemistry, Weizmann Institute of Science, IL-76100, Reovot, Israel

First Published:January2009

PLEASE SCROLL DOWN FOR ARTICLE

INVITED ARTICLE

Atomization energies of the carbon clusters C_n ($n = 2-10$) revisited by means of W4 theory as well as density functional, Gn, and CBS methods

Amir Karton, Alex Tarnopolsky and Jan M.L. Martin*

Department of Organic Chemistry, Weizmann Institute of Science, IL-76100 Reḥovot, Israel

The thermochemistry of the carbon clusters C_n ($n = 2-10$) has been revisited by means of W4 theory and W3.2lite theory. Particularly, the larger clusters exhibit very pronounced post-CCSD(T) correlation effects. Despite this, our best calculated total atomization energies agree surprisingly well with the 1991 estimates obtained from scaled CCD(ST)/6-31G* data. Accurately reproducing the small singlet–triplet splitting in C_2 requires inclusion of connected quintuple and sextuple excitations. Post-CCSD(T) correlation effects in C_4 stabilize the linear form. Linear/cyclic equilibria in C_6, C_8, and C_{10} are not strongly affected by connected quadruples, but they are affected by higher-order triples, which favor polyacetylenic rings but disfavor cumulenic rings. Near the CCSD(T) basis set limit, C_{10} does undergo bond angle alternation in the bottom-of-the-well structure, although it is expected to be absent in the vibrationally averaged structure. The thermochemistry of these systems, and particularly the longer linear chains, is a particularly difficult test for density functional methods. Particularly for the smaller chains and the rings, double-hybrid functionals clearly outperform conventional DFT functionals for these systems. Among compound thermochemistry schemes, G4 clearly outperforms the other members of the Gn family. Our best estimates for total atomization energies at 0 K are: $C_2(^1\Sigma_g^+)$ 144.07, $C_2(^3\Pi_u)$ 142.39, $C_3(^1\Sigma_g^+)$ 315.83, $C_4(^3\Sigma_g^-)$ 429.16, $C_4(^1A_g)$ 430.09, $C_5(^1\Sigma_g^+)$ 596.64, $C_6(^3\Sigma_g^-)$ 717.19, $C_6(^1A_1')$ 729.68, $C_7(^1\Sigma_g^+)$ 877.45, $C_8(^3\Sigma_g^-)$ 1001.86, $C_8(^1A_g)$ 1014.97, $C_9(^1\Sigma_g^+)$ 1159.21, $C_{10}(^3\Sigma_g^-)$ 1288.22, and $C_{10}(^1A_1')$ 1355.54 kcal mol^{-1}.

Keywords: thermochemistry; *ab initio*; anharmonic force fields; density functional theory

1. Introduction

Carbon clusters, C_n, are, on the one hand, precursors for diamond films generated by CVD (chemical vapor deposition), and, on the other, the smaller congeners of fullerenes and carbon nanotubes. Their chemistry has been reviewed, among others, by Van Orden and Saykally [1], by Lifshitz [2], and, most recently, in the Introduction to Ref. [3].

One of the earliest papers to offer a coherent picture of chemical bonding in the C_n clusters for lower n was the seminal study of Raghavachari and Binkley (RB) [4]. While based on what by present-day standards are fairly primitive calculations (HF/6-31G* optimizations and frequency calculations accompanied by CCD(ST)/6-31G* single-point energy evaluations), RB established a number of key features of the chemistry of these systems. This work was expanded upon to some degree by Hutter, Lüthi, and Diederich (HLD) [5], who carried out DFT optimizations and frequency calculations through C_{18}, and by Martin and Taylor (MT1) [6], who carried out CCSD(T) coupled cluster optimizations and harmonic frequency calculations with fairly modest basis sets, reviewed the experimental information available at this point, and proposed a number of reassignments of infrared spectroscopic features. Guided by predictions in this latter study, cyclic C_6 [7] and C_8 [8] were experimentally discovered in graphite vapor trapped in a solid argon matrix. (The first experimental evidence for nonlinear small carbon clusters was probably the Coulomb explosion experiments carried out at the Weizmann Institute [9].)

Earlier, linear C_4 and C_5 were correctly assigned [10] following computational predictions [11], and the characterization of linear C_6 likewise involved an interplay between theory [12] and experiment [13]. Linear C_7 and C_9 were discovered [14] following computational predictions [12].

As discussed by RB and MT1, the odd-numbered clusters C_{2n+1} have linear structures with closed-shell $^1\Sigma_g^+$ ground states, while for the even-numbered clusters, linear structures in $^3\Sigma_g^-$ ground states are energetically close to closed-shell singlet

---

*Corresponding author. Email: gershom@weizmann.ac.il

ring structures. Among the latter, the C_{4n+2} rings are cumulenic with $D_{(2n+1)h}$ symmetry and exhibit twin aromatic systems (one conventional, another in-plane): while the ring strain on the in-plane system in C_6 is simply too great and leads to both alternating-angle distortion and the ring being less stable than the chain. C_{10} is the first carbon cluster for which the ring structure is more stable than the chain. As for the C_{4n} clusters, while the diamond-shaped C_4 ring is nearly isoenergetic with the chain [15,16], the C_8 ring is polyacetylenic and exhibits both bond length and bond angle alternation (C_{4h} symmetry), and larger C_{4n} rings were predicted [17] to generally have polyacetylenic $C_{(2n)h}$ structures. At some point for high $4n+2$, Peierls distortion will set in: this issue has been discussed and reviewed at length in Ref. [3].

Thermochemistry was addressed in a number of theoretical and experimental studies. RB applied an empirical scaling factor of 1.1 to their CCD(ST)/ 6-31G* atomization energies, which they derived from the ratio between their calculated values and Knudsen effusion measurements by Drowart *et al.* (DBDI) [18] for C_2 through C_5. Since the DBDI values for C_4 and C_5 were third-law extrapolations based on very crude estimates of the molecular constants, the scaled estimates of RB were biased upwards, and the scaling factor required downward revision to 1.082 [19]. Later, new measurements by Gingerich and coworkers [20] became available, which also covered C_6 and C_7. Subsequently, Martin and Taylor (MT2) [21] proposed revised estimates based on CCSD(T)/cc-pVTZ and CCSD(T)/cc-pVQZ calculations with empirical basis set incompleteness corrections.

Both computational chemistry in general, and computational thermochemistry in particular, have come a long way since this time. In particular, our group recently developed a post-CCSD(T) computational thermochemistry protocol known as W4 theory [22], which exhibits an RMSD deviation from experiment (Active Thermochemical Tables, ATcT [23], values) of just $0.08 \, \text{kcal mol}^{-1}$, implying a 95% confidence interval of just $0.16 \, \text{kcal mol}^{-1}$. The purpose of the present paper is to furnish the best thermochemistry for the lower C_n clusters feasible with current technology.

Carbon clusters are among the manifold research interests of Prof. Henry F. Schaefer III [24–28], who is being honored by the present issue.

2. Computational methods

The self-consistent field (SCF), ROCCSD and ROCCSD(T) calculations [29] were carried out using

version 2006.1 of the Molpro program system [30]. All single-point post-CCSD(T) calculations were carried out using an OpenMP-parallel version of Mihály Kállay's general coupled cluster code MRCC [31] interfaced to the Austin–Mainz–Budapest version of the ACES II program system [32]. The diagonal Born–Oppenheimer correction (DBOC) calculations were carried out using the Austin–Mainz–Budapest version of the ACES II program system as well as using PSI3 [33].

For the lower-cost methods W2.2 and W3.2lite we used reference geometries optimized at the B3LYP/ cc-pVTZ level of theory, while for the more rigorous methods W3.2, W4lite, and W4 we used CCSD(T)/ cc-pVQZ reference geometries. The optimized geometries are summarized in Table 1.

For the large-scale SCF, CCSD, CCSD(T), and post-CCSD(T) single-point calculations, we employed the cc-pVnZ basis set [34]. In core–valence correlation calculations, the core–valence weighted correlation consistent basis sets of Peterson and Dunning were employed [35]. Scalar relativistic calculations were carried out using the Pacific Northwest National Laboratory (PNNL) Douglas–Kroll–Hess relativistically contracted correlation basis sets [36].

The ROHF-SCF contribution is extrapolated using the Karton–Martin [37] modification of Jensen's extrapolation formula [38]. All other extrapolations are carried out using the $A + B/L^{\alpha}$ two-point extrapolation formula (where L is the highest angular momentum present in the basis set). The ROCCSD valence contribution is partitioned into singlet-pair energies, triplet-pair energies and $\hat{T}_1$ terms [39]. The singlet- and triplet-pair energies are extrapolated with $\alpha_S = 3$ and $\alpha_T = 5$, respectively, while the $\hat{T}_1$ term (which exhibits very weak basis set dependence) is simply set equal to that in the largest basis set. All other extrapolations are carried out with $\alpha = 3$ [22,40].

The Wn family of methods W1, W2.2, W3.2lite, W3.2, W4lite, and W4 used in the present study provide a sequence of converging computational thermochemistry protocols. A detailed description and rationalization of the Wn protocols is given elsewhere [22,41–44]. For the purpose of the present paper we use the Wnh variants of the Wn methods, in which the diffuse functions are omitted from carbon and less electronegative elements [42]. (For the present all-carbon systems, this approximation is of no thermochemical consequence, but computer resource requirements are substantially reduced.) In W4h theory the SCF and valence CCSD contributions to the TAE are extrapolated from cc-pV5Z and cc-pV6Z basis sets, and the valence parenthetical triples (T)

Table 1. Theoretical geometries (in Ångstroms and degrees). In the linear systems, bond lengths are numbered from the outside in.

			r_1	r_2	r_3	r_4	r_5	α
B3LYP/pc-2	$C_2(^1\Sigma_g^+)$	$D_{\infty h}$	1.247					
	$C_2(^3\Pi_u)$	$D_{\infty h}$	1.302					
	$C_2(^3\Sigma_g^-)$	$D_{\infty h}$	1.367					
	$C_3(^1\Sigma_g^+)$	$D_{\infty h}$	1.288					
	$C_4(^3\Sigma_g^-)$	$D_{\infty h}$	1.306	1.287				
	$C_5(^1\Sigma_g^+)$	$D_{\infty h}$	1.282	1.279				
	$C_6(^3\Sigma_g^-)$	$D_{\infty h}$	1.296	1.284	1.271			
	$C_7(^1\Sigma_g^+)$	$D_{\infty h}$	1.282	1.284	1.269			
	$C_8(^3\Sigma_g^-)$	$D_{\infty h}$	1.291	1.286	1.270	1.277		
	$C_9(^1\Sigma_g^+)$	$D_{\infty h}$	1.281	1.286	1.267	1.273		
	$C_{10}(^3\Sigma_g^-)$	$D_{\infty h}$	1.288	1.287	1.269	1.277	1.270	
	$C_4(^1A_g)$	D_{2h}	1.442					117.6
	$C_6(^1A_1')$	C_{3h}	1.319					147.9
	$C_8(^1A_g)$	D_{4h}	1.252	1.380				162.1
	$C_{10}(^1A_1')$	D_{5h}	1.288					161.8
CCSD(T)/cc-pVQZ	$C_2(^1\Sigma_g^+)$	$D_{\infty h}$	1.2400[a]					
	$C_2(^3\Pi_u)$	$D_{\infty h}$	1.3153					
	$C_2(^3\Sigma_g^-)$	$D_{\infty h}$	1.3728					
	$C_3(^1\Sigma_g^+)$	$D_{\infty h}$	1.2981					
	$C_4(^3\Sigma_g^-)$	$D_{\infty h}$	1.3140	1.2936				
	$C_5(^1\Sigma_g^+)$	$D_{\infty h}$	1.2936	1.2857				
	$C_6(^3\Sigma_g^-)$	$D_{\infty h}$	1.3052	1.2905	1.2780			
	$C_7(^1\Sigma_g^+)$	$D_{\infty h}$	1.2933	1.2901	1.2759			
	$C_8(^3\Sigma_g^-)$	$D_{\infty h}$	1.3010	1.2923	1.2767	1.2832		
	$C_9(^1\Sigma_g^+)$	$D_{\infty h}$	1.2930	1.2928	1.2745	1.2799		
	$C_4(^1A_g)$	D_{2h}	1.4492					117.09
	$C_6(^1A_1')$	D_{3h}	1.3282					148.79
	$C_8(^1A_g)$	C_{4h}	1.2592	1.3926				162.74
	$C_{10}(^1A_1')$	D_{5h}	1.2940					158.25
	$C_{10}(^1A_1')$	D_{10h}	1.2914					[144.00]

[a]Fixed reference geometry used for consistency with earlier post-W4 work [40]. Actual CCSD(T)/cc-pVQZ bond distance is 1.2458 Å. W4 TAE_e at that geometry is 143.87 kcal mol^{-1}, just 0.01 kcal mol^{-1} higher than at 1.24 Å.

contribution from cc-pVQZ and cc-pV5Z basis sets. The higher-order connected triples, $\hat{T}_3 - (T)$, valence correlation contribution is extrapolated from the cc-pVDZ and cc-pVTZ basis sets. As for the connected quadruple, $\hat{T}_4$, term – the (Q) and $T_4 - (Q)$ corrections are calculated with the cc-pVTZ and cc-pVDZ basis sets, respectively, both scaled by 1.1. This formula offers a very reliable as well as fairly cost-effective estimate of the basis set limit $\hat{T}_4$ contribution [22,40]. The $\hat{T}_5$ contribution is calculated using the *sp* part of the cc-pVDZ basis set, denoted cc-pVDZ(no d). The CCSD(T) inner-shell contributions are extrapolated from cc-pwCVnZ basis sets ($n = $ T, Q). Scalar relativistic contributions (second-order Douglas–Kroll–Hess approximation [45]) are obtained from the difference between non-relativistic CCSD(T)/cc-pVQZ and CCSD(T)/cc-pVQZ-DK calculations. Atomic and molecular first-order spin–orbit coupling terms are taken from the experimental fine structure.

Finally, the DBOC is calculated at the ROHF/cc-pVTZ level of theory.

When considering the Wn sequence, it may be helpful to keep the following points in mind: (a) W1 and W2.2 completely neglect post-CCSD(T) correlation effects; (b) the difference between W1 and W2.2 is (in the context of this paper) principally a matter of more reliable CCSD(T) basis set limits and the DBOC; (c) the only differences between W2.2, on the one hand, and W3.2lite and W3.2, on the other, is the post-CCSD(T) corrections, the former with a cost-saving empirical approximation; (d) the only difference between W3.2 and W4lite is a more reliable basis set limit for the CCSD(T) part; (e) the only improvement in W4 relative to W4lite is a more rigorous account for connected quadruple and higher excitations.

All density functional results were obtained by means of a locally modified version of Gaussian 03 [46].

Table 2. Diagnostics for importance of non-dynamical correlation.

| | %TAE$_e$ | | | | CCSD/cc-pVTZ | | | | |
| | | | | | Diagnostic | | | NO occupations | |
	[SCF][a]	[(T)][a]	[post-CCSD(T)][a]	[$T_4 + T_5$][a]	$\mathcal{T}_1$	D_1	Largest T_2 amplitudes	HDOMO[b]	LUMO
$C_2(^1\Sigma_g^+)$	12.61	13.29	0.28	1.79	0.038	0.086	0.29	1.629	0.362
$C_2(^3\Pi_u)$	50.56	6.51	0.85	1.02	0.020	0.039	0.12	1.934	0.084
$C_2(^3\Sigma_g^-)$	67.70	3.40	0.53	0.34	0.011	0.021	0.08 (×2)	1.933	0.044
$C_3(^1\Sigma_g^+)$	64.88	5.52	0.30	0.64	0.023	0.052	0.10 (×2)	1.913 (×2)	0.074 (×2)
$C_4(^3\Sigma_g^-)$	66.09	4.61	0.30	0.62	0.018	0.035	0.07 (×2)	1.915 (×2)	0.068 (×2)
$C_4(^1A_g)$	64.44	4.70	0.10	0.54	0.015	0.034	0.09	1.908	0.074
$C_5(^1\Sigma_g^+)$	66.64	5.37	0.14	0.60	0.024	0.060	0.09 (×2)	1.903 (×2)	0.084 (×2)
$C_6(^3\Sigma_g^-)$	66.73	4.79	0.10	0.54	0.023	0.050	0.08	1.912 (×2)	0.074 (×2)
$C_6(^1A_1)$	64.19	5.00	0.03	0.52	0.035	0.116	0.07 (×2)	1.915 (×2)	0.098
$C_7(^1\Sigma_g^+)$	67.18	5.30	0.19	0.71	0.025	0.066	0.09 (×2)	1.897 (×2)	0.090 (×2)
$C_8(^3\Sigma_g^-)$	67.22	4.80	0.20	0.67	0.025	0.061	0.08	1.904 (×2)	0.0866 (×2)
$C_8(^1A_g)$	66.15	4.46	0.43	0.69	0.039	0.130	0.06 (×2)	1.889[d]	0.100[d]
$C_9(^1\Sigma_g^+)$	67.59	5.18	0.29	0.83	0.025	0.071	0.08 (×2)	1.895 (×2)	0.096 (×2)
$C_{10}(^3\Sigma_g^-)$	67.58	4.87	N/A	N/A	0.026	0.071	0.05 (×2)	1.901 (×2)	0.907 (×2)
$C_{10}(^1A_1')D_{5h}$	67.95	4.68	N/A	N/A	0.037	0.112	0.07 (×2)	1.900 (×2)[c,d]	0.089 (×2)[c,d]

[a]Percentages of the total atomization energy relate to non-relativistic, clamped-nuclei values with inner shell electrons constrained to be doubly occupied (C_2–C_5 from W4 theory, C_6 and C_7 from W3.2 theory, C_8 and C_9 from W3.2lite theory, C_{10} from W2.2 theory).
[b]Highest doubly occupied molecular orbital.
[c]HOMO-1: 1.904 (×2), LUMO + 1: 0.075 (×2).
[d]cc-pVDZ basis set.

3. Results and discussion

Diagnostics for the importance of non-dynamical correlation can be found in Table 2. These include the $\mathcal{T}_1$ and $\mathcal{D}_1$ diagnostics [47,48], the largest T_2 amplitudes at the CCSD/cc-pVTZ level, the HOMO and LUMO natural orbital occupations at the same level, and percentages of the total atomization energy accounted for at the SCF level, by parenthetical triples (shown elsewhere [22] to be a more reliable predictor of the importance of post-CCSD(T) correlation effects than any other diagnostic), and by post-CCSD(T) correlation effects.

Table 3 presents component breakdowns for the W3.2lite results, Table 4 for the W4 results (C_2 through C_5 only), and Table 5 a comparison between theoretical and experimental estimates for C_2 through C_{10}.

For C_2, a well-known 'problem molecule' [27,49, 50], an ATcT value is available [51]: our W4 calculation agrees with it to within overlapping uncertainties. Still higher-level W4.3 and W4.4 calculated values are in basically perfect agreement with the ATcT value [22,40]. At the W4 level, the calculated singlet–triplet splitting is found to be 609 cm^{-1}, somewhat lower than the experimental value [52] of 716 cm^{-1} (2.05 kcal mol^{-1}). Increasing the level of theory to W4.2 has

a negligible effect on the triplet state (which has much weaker multireference character) but stabilizes the singlet state by a small but significant amount. As a result, at the W4.2 level the splitting goes up to 662 cm^{-1} – the difference with W4 is entirely due to higher-order T_3 effects in the core–valence term. Further 'ramping up' to the W4.3 level sees a slight destabilization of the triplet state (mostly due to the $T_3 - (T)$ and T_4 contributions being calculated with larger basis sets), but a somewhat more pronounced stabilization of the singlet state due to quintuple and sextuple excitations. Consequently, perfect agreement with experiment is reached, with an energy difference of 2.05 kcal mol^{-1}, or 2.00 kcal mol^{-1} if the experimental spin–orbit coupling constant [52], $A = -15.25$ cm^{-1}, is taken into account. (It is not entirely clear whether the experimental $T_e = 716$ cm^{-1} refers to the lowest spin–orbit component of the triplet state or to the average of the three spin–orbit components. Incidentally, our calculated $A = -14.39$ cm^{-1} using the same procedure as in Ref. [53].) For the isoelectronic BN diatomic – which exhibits even more pathological non-dynamical correlation effects – we likewise found [53] that reproduction of the very small singlet–triplet splitting required accounting for

Table 3. Component breakdown of the final W2.2 and W3.2lite total atomization energies at the bottom of the well (in kcal mol^{-1}) obtained from B3LYP/cc-pVTZ reference geometries.

	SCF	Valence CCSD	Valence (T)	$\hat{T}_3-$(T)	$1.1 \times$(Q) /cc-pVDZ	Inner shell	Relativ.	Spin–orbit	DBOC	(a)	TAE$_e$ W2.2	TAE$_e$ W3.2lite
$C_2(^1\Sigma_g^+)$	18.30	107.60	19.39	−2.25	2.95	1.01	−0.17	−0.17	0.03	0.04	145.99	146.70
$C_2(^3\Pi_u)$	73.36	60.22	9.19	−0.17	1.08	0.96	−0.09	−0.17	0.01	0.03	143.48	144.41
$C_2(^3\Sigma_g^-)$	86.79	36.07	4.27	0.39	0.32	0.67	−0.07	−0.17	0.00	0.03	127.56	128.28
$C_3(^1\Sigma_g^+)$	207.96	93.01	17.24	−0.96	1.65	2.07	−0.19	−0.25	0.02	0.06	319.87	320.59
$C_4(^3\Sigma_g^-)$	288.48	125.46	19.76	−1.14	1.99	3.21	−0.33	−0.34	−0.29	0.08	435.95	436.84
$C_4(^1A_g)$	281.76	133.58	20.08	−1.74	1.98	2.41	−0.29	−0.34	0.03	0.08	437.23	437.51
$C_5(^1\Sigma_g^+)$	404.38	167.41	31.90	−2.51	4.01	4.62	−0.47	−0.42	0.07	0.10	607.50	609.05
$C_6(^3\Sigma_g^-)$	485.83	204.97	34.30	−2.86	4.20	5.86	−0.62	−0.51	−0.17	0.12	729.65	731.06
$C_6(^1A_1)$	476.56	227.68	36.67	−3.32	4.13	6.84	−0.87	−0.51	0.06	0.13	746.43	747.29
$C_7(^1\Sigma_g^+)$	599.93	242.14	46.43	−4.04	6.79	7.22	−0.76	−0.59	0.11	0.19	894.49	897.34
$C_8(^3\Sigma_g^-)$	683.35	282.36	48.82	−4.79	6.80	8.50	−0.92	−0.68	−0.10	0.16	1021.33	1023.43
$C_8(^1A_g)$	681.28	298.24	45.97	−2.62	7.06	9.53	−1.16	−0.68	0.09	0.17	1033.28	1037.80
$C_9(^1\Sigma_g^+)$	795.86	317.23	61.02	−6.44	9.79	9.83	−1.06	−0.76	0.15	0.19	1182.27	1185.72
$C_{10}(^3\Sigma_g^-)$	880.78	359.06	63.43	N/A	N/A	11.13	−1.21	−0.85	−0.02	0.21	1312.32	N/A
$C_{10}(^1A_1)$	934.19	376.34	64.38	N/A	N/A	12.60	−1.46	−0.85	−0.01	0.21	1385.20	N/A
Linear–cyclic isomerization energies												
$C_4(^1A_g) \rightarrow C_4(^3\Sigma_g^-)$	−6.72	8.12	0.32	−0.60	−0.01	−0.80	0.04	0.00	0.32	0.01	1.29	0.67
$C_6(^1A_1) \rightarrow C_6(^3\Sigma_g^-)$	−9.27	22.71	2.37	−0.46	−0.07	0.98	−0.25	0.00	0.23	0.00	16.77	16.24
$C_8(^1A_g) \rightarrow C_8(^3\Sigma_g^-)$	−2.07	15.88	−2.86	2.17	0.26	1.03	−0.24	0.00	0.19	0.00	11.94	14.37
$C_{10}(^1A_1') \rightarrow C_{10}(^3\Sigma_g^-)$	53.41	17.28	0.95	N/A	N/A	1.48	−0.25	0.00	0.01	N/A	72.88	N/A
Isodesmic reaction energies												
$2C_5 \rightarrow C_7 + C_3$	0.86	−0.32	0.12	−0.03	−0.42	−0.05	0.01	0.00	0.01	−0.05	0.62	0.17
$2C_6 \rightarrow C_8 + C_4$	−0.17	2.11	0.02	0.22	−0.39	0.01	0.00	0.00	0.05	0.00	2.02	1.85
$2C_7 \rightarrow C_9 + C_5$	−0.37	−0.36	−0.05	0.87	−0.22	0.00	0.00	0.00	0.01	0.09	−0.73	−0.08
$2C_8 \rightarrow C_{10} + C_6$	0.09	0.70	−0.09	N/A	N/A	0.01	0.00	0.00	−0.01	0.00	0.70	N/A
$3C_5 \rightarrow C_9 + 2C_3$	1.35	−1.01	0.20	0.82	−1.05	−0.11	0.02	0.00	0.02	0.00	0.48	0.25

(a) Difference between the ACES II and MOLPRO definitions of the valence ROCCSD(T).

connected sextuple and especially quintuple excitations, contributions of which have similar magnitudes as in C_2. For the sake of completeness, our computed T_e for the b $^3\Sigma_g^-$ state is 18.16 kcal mol^{-1} at the W4 level and 18.44 kcal mol^{-1} at the W4.3 level, compared to an experimental value [52] of 18.40 kcal mol^{-1}. Once again, essentially all post-W4 change is due to the pathological singlet state.

Perusing both Tables 3 and 4, it becomes evident that higher-order correlation effects wax increasingly more prominent as n goes up. This phenomenon is illustrated graphically in Figure 1. For example, higher-order triples for C_9 reduce TAE by 6.4 kcal mol^{-1}, while connected quadruples will increase it by approximately 9.8 kcal mol^{-1}. While these two effects partially compensate each other, together this still amounts to an n-particle truncation error at the CCSD(T) level of about 3.4 kcal mol^{-1}. For comparison, the same effect is just 0.7 kcal mol^{-1} (W3.2lite) or

1.0 kcal mol^{-1} (W4) for C_3, and 0.8 kcal mol^{-1} (W3.2lite) for C_6.

Connected quintuples likewise increase in importance as n grows, reaching nearly 1 kJ mol^{-1} for C_5 (the largest system for which we were able to calculate their contribution explicitly).

Interestingly enough, with the anomalous exception of $C_2(^1\Sigma_g^+)$, all molecules considered here have %TAE[(T)] diagnostics hovering in the 5% range, which indicates moderate but not severe non-dynamical correlation [22].

We also note that the very small linear–cyclic energy difference in C_4 has an appreciable post-CCSD(T) contribution: at the W4 level, higher-order connected triples and connected quadruples favor the linear structure by 0.5 and 0.4 kcal mol^{-1}, respectively. Likewise, in C_6, higher-order triples favor the linear structure by 0.5 kcal mol^{-1} (W3.2) while connected quadruples only affect the equilibrium by 0.08 kcal

Table 4. Component breakdown of the final W4^c total atomization energies at the bottom of the well (in kcal mol^{-1}) obtained from CCSD(T)/cc-pVQZ reference geometries.

	SCF	Valence CCSD	Valence (T)	$\hat{T}_3-(T)$	$\hat{T}_4$ (c)	$\hat{T}_5$	$\hat{T}_6$	Inner shell	Relativ.	Spin–orbit	DBOC	(a)	(b)	TAE$_e$^{a}
C$_2$($^1\Sigma_g^+$)	18.38	107.60	19.37	−2.19	2.37	0.24	[0]	1.06	−0.17	−0.17	0.03	0.04	0	146.52
ditto W4.3	18.38	107.60	19.37	−2.24	2.35	0.32	0.07	1.25	−0.17	−0.17	0.03	0.00	0	146.78
C$_2$($^3\Pi_u$)	72.87	60.65	9.39	−0.25	1.33	0.14	[0]	0.89	−0.09	−0.17	0.01	0.03	0.05	144.78
ditto W4.3	72.87	60.65	9.39	−0.27	1.29	0.12	0.01	0.92	−0.09	−0.17	0.01	0.00	0.05	144.72
C$_2$($^3\Sigma_g^-$)	86.62	36.29	4.35	0.25	0.41	0.03	[0]	0.64	−0.07	−0.17	0.00	0.03	0.00	128.36
ditto W4.3	86.62	36.29	4.35	0.22	0.42	0.03	0.001	0.65	−0.07	−0.17	0.00	0.00	0.00	128.34
C$_3$($^1\Sigma_g^+$)	207.18	93.58	17.63	−1.10	2.07	−0.02	[0]	1.96	−0.19	−0.25	0.02	0.06	0	320.90
C$_4$($^3\Sigma_g^-$)	287.62	126.19	20.06	−1.37	2.56	0.12	[0]	3.08	−0.34	−0.34	−0.35	0.08	0.33	437.28
C$_4$(^1A_g)	280.97	134.15	20.48	−1.91	2.16	0.19	[0]	2.28	−0.29	−0.34	0.03	0.08	0	437.77
C$_5$($^1\Sigma_g^+$)	403.09	168.48	32.47	−2.75	3.39	0.21^b	[0]	4.42	−0.48	−0.42	0.07	0.10	0	608.54
C$_6$($^3\Sigma_g^-$)^c	484.46	206.00	34.80	−3.19	3.92	N/A	[0]	5.71	−0.64	−0.51	−0.23	0.12	N/A	715.89
C$_6$($^1A_1'$)^c	475.87	228.16	37.07	−3.60	3.85	N/A	[0]	6.58	−0.88	−0.51	0.06	0.13	N/A	729.68
C$_7$($^1\Sigma_g^+$)^c	589.19	243.37	47.20	−4.68	6.37	N/A	[0]	6.96	−0.78	−0.59	0.12	0.15	0	896.22
				Singlet–triplet and linear–cyclic energy differences										
C$_2$(X$^1\Sigma_g^+$) → C$_2$(a $^3\Pi_u$)	−54.49	46.95	9.98	−1.94	1.04	0.10	[0]	0.17	−0.08	0	0.01	0.01	−0.05	1.74
ditto W4.3	−54.49	46.95	9.98	−1.96	1.06	0.20	0.06	0.33	−0.08	0	0.01	0	−0.05	2.05^d
C$_2$(X$^1\Sigma_g^+$) → C$_2$($^3\Sigma_g^-$)	−68.24	71.31	15.02	−2.44	1.96	0.21	[0]	0.41	−0.10	0	0.02	0.01	0.00	18.16
ditto W4.3	−68.24	71.31	15.02	−2.46	1.93	0.29	0.07	0.59	−0.10	0	0.02	0	0.00	18.44^e
C$_4$(^1A_g) → C$_4$($^3\Sigma_g^-$)	−6.64	7.96	0.41	−0.54	−0.40	0.07	[0]	−0.80	0.05	0	0.38	0.01	−0.33	0.49
C$_6$($^1A_1'$) → C$_6$($^3\Sigma_g^-$)	−8.60	22.16	2.27	−0.41	−0.08	N/A	[0]	0.87	0.24	0	0.29	0.00	N/A	16.26

(a) Difference between the ACES II and MOLPRO definitions of the valence ROCCSD(T).
(b) RCCSDTQ/cc-pVDZ−UCCSDTQ/cc-pVDZ.
(c) UHF reference: for RCCSDTQ−UCCSDTQ, cfr. (b).
^{a}Note that the TAE$_e$ do not include ΔDBOC.
^{b}$\hat{T}_5$ approx. as CCSDTQ(5)$_\Lambda$/cc-pVDZ(no d)−CCSDTQ/cc-pVDZ(no d).
^{c}C$_6$ and C$_7$ from W3.2 theory.
^{d}Experimental value: 2.05 kcal mol^{-1} [52].
^{e}Experimental value: 18.40 kcal mol^{-1} [52].

mol^{-1} (favoring the ring). In polyacetylenic C$_8$, however, higher-order triples favor the ring by 2 kcal mol^{-1}, while the effect of connected quadruples is nearly an order of magnitude smaller. This raises the question whether a general trend exists: higher-order triples favoring polyacetylenic rings over linear structures while favoring linear over cumulenic ring structures. Unfortunately, CCSDT calculations beyond C$_8$ are beyond our computational resources.

The equilibrium structure of the C$_{10}$ ring displays clear angle alternation. It was previously noted [6] that the barrier towards the D$_{10h}$ saddle point is very small, and there has been some speculation (e.g., Refs. [25,54–56]) that it might actually disappear at the basis set limit. Our calculated CCSD(T)/cc-pVTZ, CCSD(T)/cc-pVQZ(no g), and CCSD(T)/cc-pVQZ barriers are 1.11, 0.48, and 0.33 kcal mol^{-1}, respectively. At the {Q, 5} basis set limit at CCSD(T)/cc-pVQZ optimum geometries, the D$_{5h}$ alternating-angles ring is 23.00 kcal mol^{-1} more stable at the SCF level than the D$_{10h}$ saddle point. CCSD valence correlation lowers this by 18.37 kcal mol^{-1} to

4.63 kcal mol^{-1}, while parenthetical triples shave off yet another 4.32 kcal mol^{-1}. These components add up to a basis set limit CCSD(T) deformation energy of 0.30 kcal mol^{-1}. MP2, as expected [6,17], grossly favors the more symmetric structure, and SCS-MP2/cc-pVQZ [57] is unable to overcome this bias, reaching −26.75 kcal mol^{-1} for the isomerization energy. At the SCS-CCSD/cc-pVQZ [58] level, however, +0.15 kcal mol^{-1} is obtained, slightly increasing to 0.18 kcal mol^{-1} at the SCS-CCSD/cc-pV5Z//CCSD(T)/cc-pVQZ level. These numbers are as close to the CCSD(T) answer as one can reasonably hope.

Notwithstanding the above, the calculated B3LYP/cc-pVTZ zero-point vibrational energy of the saddle point is about 1 kcal mol^{-1} smaller than for the D$_{5h}$ minimum. This implies that the vibrationally averaged structure will have D$_{10h}$ symmetry even at 0 K.

Inner-shell correlation contributions become fairly hefty for the larger clusters, reaching 12.6 kcal mol^{-1} for C$_{10}$. For the linear C$_n$ clusters, these contributions
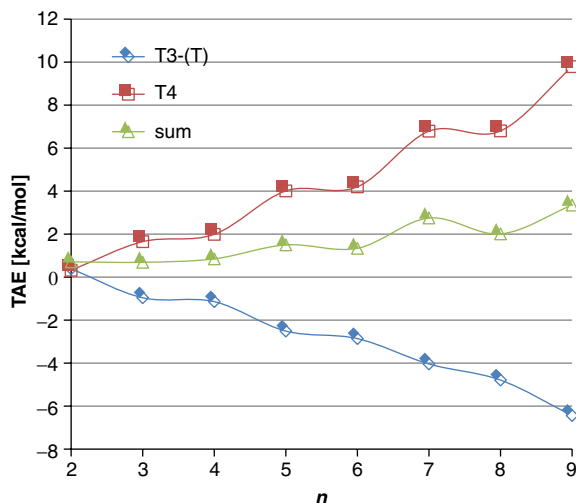
Figure 1. $\hat{T}_3 - (T)$ and $\hat{T}_4$ contributions to the total atomization energies for the linear C_n clusters (from W3.2lite theory, in kcal mol^{-1}).

scale almost perfectly linearly with n. For C_6, C_8, and C_{10}, inner-shell correlation systematically favors the cyclic structures: the somewhat anomalous bicyclic C_4 structure does not follow this trend.

It was earlier noted by RB, for the linear clusters, that the reactions $2C_n \rightarrow C_{n+2} + C_{n-2}$ are nearly thermoneutral at their level of theory. We do find the same to be the case at the W3.2lite level: however, relative to the (quite small) overall reaction energies, the post-CCSD(T) contributions are still non-negligible. If we assume that those reaction energies are converged at the W3.2lite level (which is probably justified to 0.5 kcal mol^{-1}, and certainly to 1 kcal mol^{-1}), we can obtain extrapolated W4 atomization energies for species heavier than C_5 (the practical limit for full W4 calculations with the presently available hardware). Our best estimates are presented in Table 5.

Perhaps the most striking feature of these numbers is the outstanding agreement between our best calculated TAE$_0$ values for the linear clusters and the earlier, empirically scaled, data of MFG. Indeed, it is hard to believe that these latter rudimentary estimates – blissfully ignorant of higher-order correlation effects, inner-shell correlation, etc. – capture so much of the thermochemistry in these systems. We note that this scaling is not transferable to the rings, for which the MFG estimates are clearly too low.

Our best values agree reasonably well with the available measured data of Gingerich and coworkers [20], considering the size of the uncertainties on the latter – although generally the calculated values are near the upper edges of the experimental error bars.

Inspection of Table 3 also suggests (not surprisingly) that, as n increases, the C_n atomization energies at the W3.2lite level are progressively greater overestimates compared to the estimated W4 numbers.

In conjunction with the ATcT revised heat of formation of the carbon atom [23, (c)], $\Delta H^\circ_{f,0}$ [C(g)] = 170.06 ± 0.026 kcal mol^{-1}, we can offer the following revised heats of formation at 0 K: $C_2(^1\Sigma_g^+)$ 196.04, $C_2(^3\Pi_u)$ 197.72, $C_3(^1\Sigma_g^+)$ 194.33, $C_4(^3\Sigma_g^-)$ 251.06, $C_4(^1A_g)$ 250.13, $C_5(^1\Sigma_g^+)$ 253.63, $C_6(^3\Sigma_g^-)$ 304.14, $C_6(^1A_1')$ 290.65, $C_7(^1\Sigma_g^+)$ 312.94, $C_8(^3\Sigma_g^-)$ 358.58, $C_8(^1A_g)$ 345.47, $C_9(^1\Sigma_g^+)$ 371.29, $C_{10}(^3\Sigma_g^-)$ 412.33, and $C_{10}(^1A_1')$ 345.01 kcal mol^{-1}.

Table 6 presents computed atomization energies, and error statistics relative to our best values, for more approximate compound thermochemistry methods such as G2MP2 [59], G2 [60], G3 [61], G3B3 [62], G4 [63], G4(MP2) [64], CBS-QB3 [65], CBS-APNO [66], W1h [41], and W2.2 for the thermochemistry of these systems.

Excluding C_8 and larger clusters (for which we deem our best calculated values to be less reliable), one sees similar error statistics for W1h and for W2.2, suggesting that an RMSD of about 1 kcal mol^{-1} is the best one can hope for without including post-CCSD(T) correlation effects. CBS-APNO and W1h have comparable RMSD errors: however, while the W1h values tend to be underestimates (consistent with the positive post-CCSD(T) correlation effects), the CBS-APNO values tend to be overestimates. The next best performer, G4, errors on both sides. Somewhat counterintuitively, G2MP2 displays marginally better error statistics than G2 – despite MP2 being clearly inappropriate for these systems – and G3 noticeably better ones than G3B3 – despite several qualitatively wrong reference geometries and spurious imaginary frequencies at the levels of theory used in G3 for reference geometries (MP2/6-31G*) and ZPVEs (HF/6-31G*), respectively. We believe the apparently better performance of G3 to be due to error compensation. CBS-QB3 clearly outperforms G3B3: in addition, it errs on the 'right' side – underestimating the best values, consistent with CCSD(T) limits. The unrealistically small linear–cyclic difference calculated for C_8 is something of a 'clinker' on the part of CBS-QB3, however. One statement we can confidently make is that, for these systems too, G4 clearly outperforms the other members of the Gn series. Performance of G4(MP2), which actually does include a CCSD(T)/6-31G(d) step but considers basis set extension effects at the MP2 level only, is considerably degraded relative to G4, rather more so than generally seen [64]. This is not surprising in light of the poor performance of MP2 for the present systems.

Table 5. Total atomization energies at 0 K (kcal mol^{-1})^a.

		ZPVE^b	W2.2	W3.2lite	W3.2	W4lite	W4	MT cc-pVTZ	cc-pVQZ	MFG	RB	Exp.^{c}	Uncert.
$C_2(^1\Sigma_g^+)$		2.64^d	143.39	144.06	143.88	143.93	143.88^e	145.1	144.2	144.8	147.1	144.6	1.9
$C_2(^3\Pi_u)$		2.34^d	141.16	142.07	141.94	141.99	142.45^f	141.1	142.4				
$C_2(^3\Sigma_g^-)$		2.09^d	125.45	126.19	126.01	126.13	126.27						
$C_3(^1\Sigma_g^+)$	lin	5.07	314.80	315.52	315.27	315.32	315.83	314.4	314.3	315.7	320.9	311.4	3.1
$C_4(^3\Sigma_g^-)$	lin	8.11	427.83	428.72	428.26	428.34	429.16	423.5	426.1			428.5	4.1
$C_4(^1A_g)$	cyc	7.68	429.55	429.83	429.52	429.60	430.09	427.7	429.3	430.3	437.6		
$C_5(^1\Sigma_g^+)$	lin	11.89	595.60	597.16	596.65	596.81	596.64	592.9	594.0	596.8	606.8	591.5	4.1
$C_6(^3\Sigma_g^-)$	lin	14.50	715.15	716.56	715.89	716.01^g	717.19^g	708.0	N/A			706.3	4.8
$C_6(^1A_1')$	cyc	16.98	729.45	730.31	729.68			720.6	724.9	722.8	734.7		
$C_7(^1\Sigma_g^+)$	lin	18.18	876.31	879.16[878.8]	878.03	878.28^h	877.45^h	870.9	[873.7]	877.7	892.4	873.1	4.8
$C_8(^3\Sigma_g^-)$	lin	20.70	1000.63	1002.73[1004.4]	1001.86^i			992.9	N/A			[984.0]	[10.4]
$C_8(^1A_g)$	cyc	22.83	1010.44	1014.97				998.9	N/A	1004.6	1021.3		
$C_9(^1\Sigma_g^+)$	lin	24.35	1157.91	1161.37[1161.2]	1160.36^j	1160.72^j	1159.21^j	1149.6	N/A	1158.4	1177.8	[1154.6]	[10.4]
$C_{10}(^3\Sigma_g^-)$	lin	26.82	1285.50	1288.22^k[1288.9]				[1277.8]	N/A				
$C_{10}(^1A_1')$	cyc	29.65	1355.54					1343.1	N/A	1344.3	1366.6		
Reaction energies (linear clusters)													
$2C_4 \rightarrow C_6 + C_2(^3\Pi_u)$			-0.80	-1.18	-1.32			-2.10					
$2C_4 \rightarrow C_6 + C_2(^3\Sigma_g^-)$			14.91	14.70	14.62								
$2C_5 \rightarrow C_7 + C_3$			0.09	-0.37	0.01			0.5				-1.43	9.9
$2C_6 \rightarrow C_8 + C_4$			1.84	1.67				-0.4					
$2C_7 \rightarrow C_9 + C_5$			-0.94	-0.20				-0.7					
$2C_8 \rightarrow C_{10} + C_6$			0.67										
$3C_5 \rightarrow C_9 + 2C_3$			-0.75	-0.94									

^{a}Reference geometries for all the W3.2lite calculations and for all clusters larger than C_7 are at the B3LYP/cc-pVTZ level of theory; values in square brackets were obtained with the formula: $TAE_0[C_n] = 2 \times TAE_0[C_{n-2}] - TAE_0[C_{n-4}]$.
^{b}The zero-point vibrational energies for C_3–C_{10} are B3LYP/pc-2 scaled by 0.985.
^{c}Ref. [20].
^{d}From $\omega_e/2 - \omega_e x_e/4$, with ω_e and $\omega_e x_e$ taken from Ref. [52].
^{e}ATcT value is 144.03 ± 0.13 kcal mol^{-1}, W4.2 value is 144.05 kcal mol^{-1} (142.46 kcal mol^{-1} for the triplet state). W4.3 and W4.4 values for the singlet state are 144.08 and 144.07 kcal mol^{-1}, respectively [40].
^{f}W4.3 value is 142.39 kcal mol^{-1}.
^{g}Estimated by assuming that the $2C_4(^3\Sigma_g^-) \rightarrow C_6(^3\Sigma_g^-) + C_2(^3\Pi_u)$ reaction energy remains unchanged at the W3.2 and post-W3.2 levels. Via $C_2(^3\Sigma_g^-)$, the estimated W4lite and W4 numbers are 715.93 and 717.43 kcal mol^{-1}, respectively.
^{h}Estimated by assuming that the $2C_5 \rightarrow C_7 + C_3$ reaction energy remains unchanged at the W3.2 and post-W3.2 levels.
^{i}Estimated by assuming that the $2C_6 \rightarrow C_8 + C_4$ reaction energy remains unchanged at the W3.2lite and W3.2 levels.
^{j}Estimated by assuming that the $3C_5 \rightarrow C_9 + 2C_3$ reaction energy remains unchanged at the W3.2lite and post-W3.2lite levels.
^{k}Estimated by assuming that the $2C_8 \rightarrow C_{10} + C_6$ reaction energy remains unchanged at the W2.2 and W3.2lite levels.

Finally, we compare the relative performance of different DFT exchange-correlation functionals in predicting the binding energies of the carbon clusters considered in the present work. As reference data we use our best available [67] non-relativistic, clamped-nuclei, zero-point exclusive TAEs. The exchange-correlation functionals employed include the following classes: (a) generalized gradient approximation (GGA): HCTH407 [68], BLYP [69,70], BPW91 [69,71], BP86 [69,72] and PBE [73]; (b) meta-GGA: M06-L [74], VSXC [75], TPSS [76] and τ-HCTH [77]; (c) hybrid GGA: PBE0 [78], B97-2 [79], B3PW91 [71,80], B97-1 [81], B98 [82], TPSSh [83], B3LYP [70,80,84], mPW1K [85,86] and BHLYP [87]; (d)

hybrid meta-GGA: mPW1B95 [86,88], B1B95 [69,89], M06 [90], PW6B95 [91], TPSS1KCIS [92], M05 [93], τ-HCTHh [77], BMK [94], M06-2X [90], BB1K [95] and PWB6K [91]; and (e) double hybrid functionals: B2-PLYP [96], mPW2-PLYP [97], B2T-PLYP [98], B2K-PLYP [98] and B2GP-PLYP [99]. Unless otherwise indicated, the pc-2 basis set of Jensen [100], which is of [4s3p2d1f] quality but optimized for Hartree–Fock and DFT calculations, was employed throughout. The root mean square deviations (RMSD), mean signed deviations (MSD), and mean average deviations (MAD) are gathered in Table 7.

In general, the GGA, meta-GGA, hybrid-GGA, and hybrid meta GGA functionals systematically

Table 6. Performance of standard composite computational thermochemistry methods. Total atomization energies at 0 K and error statistics with respect to our best values (in kcal mol^{-1}).

	G2MP2	G2	G3	G3B3	CBS-QB3	CBS-APNO	G4	G4(MP2)	W1h	W2.2	Best estimate [67]
$C_2(^1\Sigma_g^+)$	146.81	146.90	146.94	147.91	144.29	144.28	147.01	148.89	143.15	143.39	144.07
$C_2(^3\Pi_u)$	140.28	140.48	142.72	143.73	140.13	140.83	142.35	143.46	141.00	141.16	142.39
$C_3(^1\Sigma_g^+)$	316.75	316.89	317.53	318.86	314.21	314.96	316.93	318.84	314.75	314.79	315.83
$C_4(^1A_g)$	430.30	430.73	428.98	430.91	427.39	430.12	431.66	433.94	429.10	429.52	430.09
$C_4(^3\Sigma_g^-)$	424.52	425.63	429.61	431.65	426.87	428.10	428.85	429.67	428.15	427.73	429.16
$C_5(^1\Sigma_g^+)$	596.95	597.50	599.98	601.87	594.52	597.19	598.34	600.44	595.71	595.58	596.64
$C_6(^1\prime)$	725.51	726.01	727.73	732.43	727.18	731.10	731.72	733.92	728.76	729.36	729.68
$C_6(^3\Sigma_g^-)$	710.69	709.14	718.39	719.34	714.86	719.04	715.19	715.87	715.44	715.10	717.19
$C_7(^1\Sigma_g^+)$	876.39	877.42	881.72	884.02	874.30	878.83	879.28	881.41	876.45	876.28	877.45
$C_8(^1A_g)$	1005.15	1005.89	1011.16	1016.63	1006.61		1013.39	1015.80	1009.80	1010.44	1014.97
$C_8(^3\Sigma_g^-)$	994.13	996.90	1004.38	1004.68	1000.48		999.09	999.66	1000.90	1000.63	1001.86
$C_9(^1\Sigma_g^+)$	1156.44	1158.01	1164.12	1166.88	1155.66		1160.51	1162.64	1158.07	1157.91	1159.21
$C_{10}(^1A_1)$	1350.14	1351.63	1359.15	1363.49	1353.80		1359.14	1361.25	1355.11	1355.54	1355.54
$C_{10}(^3\Sigma_g^-)$	1277.31	1280.91	1290.12	1289.43	1284.83		1283.48	1283.95	1285.72	1285.50	1288.22
RMSD	5.39	4.49	2.79	4.22	3.22		2.30	3.45	1.83	1.76	
RMSD[a]	4.65	4.22	2.77	3.92	3.30		1.80	3.11	1.84	1.73	
RMSD[b]	3.25	3.41	2.29	3.58	2.27	1.16	1.73	3.31	1.14	1.17	
RMSD[c]	3.31	3.48	2.21	3.55	2.41	1.22	1.51	3.07	1.17	1.22	

[a]RMSD w/o C_{10}.
[b]RMSD w/o C_8–C_{10}.
[c]RMSD w/o C_8–C_{10} and $C_2(^1\Sigma_g^+)$.

overestimate the binding energies and lead to unacceptable RMSDs of 11–57 kcal mol^{-1}, while the so-called 'kinetics' functionals (HF exchange $> 40\%$) BHLYP, mPW1K, PWB6K, BB1K, and to a lesser extent BMK tend to systematically underestimate the binding energies.

Not quite surprisingly, all conventional DFT functionals fare rather poorly, with RMSDs in the double digits overall. Simply eliminating the pathological C_2 singlet case brings RMSD below 10 kcal mol^{-1} for four functionals: M05, BB1K, M06-2X, and BMK (9.4, 8.4, 7.5, and 6.2 kcal mol^{-1}, respectively). Interestingly, once the linear systems larger than C_4 (and the C_{10} ring) are also eliminated, RMSDs drop sharply almost across the board. Long cumulenic chains are expected to be a 'torture test' for any DFT method.

This becomes especially clear for the double hybrids. Near the basis set limit, RMSD for the reduced set of systems actually reaches the 2 kcal mol^{-1} range that can generally be expected for functionals like B2GP-PLYP [99]. For the long chains, however, severe overestimates set in. We note that these systems have increasingly narrower HOMO–LUMO gaps, and that [101] they have exceptionally large electron affinities for large n. It is perhaps not overly surprising that systems that put even post-CCSD(T) methods severely to the test (and, for instance, have connected quadruples contributions that climb to 10 kcal mol^{-1}

for C_9) would be beyond the reach of double hybrids, let alone conventional DFT functionals.

In terms of singlet–triplet equilibria, as noted earlier [102], shortcomings of conventional DFT functionals (and particularly 'kinetics' functionals) are exacerbated by a natural bias of hybrid functionals towards high-spin states. This issue is mitigated by the MP2-like correlation in double hybrids.

4. Conclusions

The thermochemistry of the carbon clusters C_n ($n = 2-10$) has been revisited by means of W4 theory and W3.2lite theory. Particularly the larger clusters exhibit very pronounced post-CCSD(T) correlation effects. Despite this, our best calculated total atomization energies agree surprisingly well with the 1991 estimates obtained from scaled CCD(ST)/6-31G* data. Accurately reproducing the small singlet–triplet splitting in C_2 requires inclusion of connected quintuple and sextuple excitations. Post-CCSD(T) correlation effects in C_4 stabilize the linear form. Linear/cyclic equilibria in C_6, C_8, and C_{10} are not strongly affected by connected quadruples, but they are affected by higher-order triples, which favor polyacetylenic rings but disfavor cumulenic ones. Near the basis set limit, C_{10} does undergo bond angle alternation in the

Table 7. Performance statistics (kcal mol^{-1}) of various exchange-correlation functionals for the carbon clusters considered in the present work.[a] Unless otherwise indicated, all calculations were done with the pc-2 basis set.

Class	Functional	RMSD	MSD	MAD	RMSD[a]	RMSD[b]
GGA	HCTH407	32.7	25.9	27.8	33.7	15.3
	BLYP	29.2	22.0	23.9	30.1	10.5
	BPW91	48.5	40.5	41.8	50.2	26.8
	BP86	60.4	51.6	52.3	62.7	35.7
	PBE	74.4	63.9	64.3	77.2	46.8
Meta GGA	M06-L	43.3	35.6	37.4	44.8	23.5
	VSXC	31.8	24.8	26.7	32.8	13.0
	TPSS	22.6	15.6	18.2	22.9	7.3
	τHCTH	27.9	21.2	23.4	28.6	11.2
Hybrid GGA	PBE0	28.1	20.1	23.9	28.3	14.1
	B97-2	25.5	18.6	21.8	25.7	11.2
	B3PW91	21.9	14.3	18.0	21.6	8.1
	B97-1	22.1	14.7	18.3	21.8	7.8
	B98	14.5	5.3	11.7	12.8	5.5
	TPSSh	12.2	1.7	9.7	10.3	7.1
	B3LYP	13.1	2.0	10.9	11.3	8.2
	mPW1K	20.2	−17.7	17.7	17.0	17.2
	BHLYP	56.6	−52.4	52.4	56.6	48.1
Hybrid meta GGA	mPW1B95	20.7	13.6	17.7	20.3	9.4
	B1B95	18.1	11.2	15.1	17.4	7.3
	M06	19.7	14.2	17.2	19.6	11.1
	PW6B95	18.1	10.9	14.9	17.4	6.3
	TPSS1KCIS	23.2	16.2	19.2	23.3	8.3
	M05	10.4	4.3	8.7	9.4	8.8
	τHCTHh	24.1	16.8	20.1	24.2	9.1
	BMK	11.8	−4.2	7.5	6.2	7.6
	M06-2X	10.5	2.5	7.7	7.5	4.2
	BB1K	12.7	−8.9	9.0	8.4	9.9
	PWB6K	14.6	−11.1	11.1	10.4	11.7
Double hybrid	B2GP-PLYP[c]	9.1	3.4	7.0	8.6	2.6
	B2GP-PLYP[d]	12.1	7.1	9.3	12.1	2.1
	B2GP-PLYP[e]	7.7	1.5	6.0	6.9	3.8
	B2GP-PLYP[f]	10.2	5.1	7.8	9.9	1.8
	B2-PLYP[c]	13.8	8.7	10.7	14.0	2.6
	B2-PLYP[d]	16.4	11.4	12.9	16.7	4.1
	B2-PLYP[e]	12.2	7.1	9.6	12.2	2.4
	B2-PLYP[f]	14.6	9.7	11.4	14.8	3.1
	B2T-PLYP[c]	9.2	3.3	7.4	8.6	3.2
	B2T-PLYP[d]	11.7	6.4	9.1	11.5	2.0
	B2T-PLYP[e]	8.0	1.5	6.5	7.2	4.3
	B2T-PLYP[f]	10.0	4.6	7.9	9.6	2.4
	B2K-PLYP[c]	7.4	0.4	5.7	6.4	4.0
	B2K-PLYP[d]	10.1	4.8	7.5	9.8	1.9
	B2K-PLYP[e]	6.7	−1.8	5.2	5.5	5.5
	B2K-PLYP[f]	8.2	2.5	6.2	7.5	2.5
	mPW2-PLYP[c]	8.1	−0.1	6.7	6.9	6.2
	mPW2-PLYP[d]	9.2	2.4	7.7	8.3	4.4
	mPW2-PLYP[e]	7.8	−1.6	5.9	6.3	7.2
	mPW2-PLYP[f]	8.3	0.8	6.9	7.2	5.4

[a]Excluding $C_2(^1\Sigma_g^+)$.
[b]Excluding $C_2(^1\Sigma_g^+)$, C_{10}, and all the linear systems larger than C_4.
[c](all electron) cc-pwCVQZ basis set.
[d](all electron) cc-pwCVQZ basis set combined with a CBS extrapolation where Nmin = 15 as recommended in Ref. [103].
[e](frozen core) pc-3 basis set.
[f](frozen core) pc-3 basis set combined with a CBS extrapolation where Nmin = 15 as recommended in Ref. [103].

bottom-of-the-well structure, although it is expected to be absent in the vibrationally averaged structure. The thermochemistry of these systems, and particularly the longer linear chains, is a particularly difficult test for density functional methods. Particularly for the smaller chains and the rings, double-hybrid functionals clearly outperform conventional DFT functionals for these systems. Among compound thermochemistry schemes, G4 clearly outperforms the other members of the Gn family. Our best estimates for total atomization energies at $0\,\mathrm{K}$ are: $C_2(^1\Sigma_g^+)$ 144.07, $C_2(^3\Pi_u)$ 142.39, $C_3(^1\Sigma_g^+)$ 315.83 $C_4(^3\Sigma_g^-)$ 429.16, $C_4(^1A_g)$ 430.09, $C^5(^1\Sigma_g^+)$ 596.64, $C_6(^3\Sigma_g^-)$ 717.19, $C_6(^1A_1')$ 729.68, $C_7(^1\Sigma_g^+)$ 877.45, $C_8(^3\Sigma_g^-)$ 1001.86, $C_8(^1A_g)$ 1014.97, $C_9(^1\Sigma_g^+)$ 1159.21, $C_{10}(^3\Sigma_g^-)$ 1288.22, and $C_{10}(^1A_1')$ 1355.54 kcal mol^{-1}.

Acknowledgements

References

[1] A. Van Orden and R.J. Saykally, Chem. Rev. **98**, 2313 (1998).

[2] C. Lifshitz, Int. J. Mass Spectrom. **200**, 423 (2000).

[3] S. Arulmozhiraja and T. Ohno, J. Chem. Phys. **128**, 114301 (2008).

[4] (a) K. Raghavachari and J.S. Binkley, J. Chem. Phys. **87**, 2191 (1987); (b) K. Raghavachari, Personal communication.

[5] J. Hutter, H.P. Lüthi, and F. Diederich, J. Am. Chem. Soc. **116**, 750 (1994).

[6] J.M.L. Martin and P.R. Taylor, J. Phys. Chem. A **100**, 6047 (1996); For a recent update, see K. Yousaf and P.R. Taylor, Chem. Phys. **349**, 58 (2008).

[7] (a) J.D. Presilla-Marquez, J.A. Sheehy, J.D. Mills, P.G. Carrick, and C.W. Larson, Chem. Phys. Lett. **274**, 439 (1997); (b) S.L. Wang, C.M.L. Rittby, and W.R.M. Graham, J. Chem. Phys. **107**, 6032 (1997).

[8] (a) S.L. Wang, C.M.L. Rittby, and W.R.M. Graham, J. Chem. Phys. **107**, 7025 (1997); (b) J.D. Presilla-Marquez, J. Harper, J.A. Sheehy, P.G. Carrick, and C.W. Larson, Chem. Phys. Lett. **300**, 719 (1999).

[9] D. Zajfman, H. Feldman, O. Heber, D. Kella, D. Majer, Z. Vager, and R. Naaman, Science **258**, 1129 (1992).

[10] (a) M. Vala, T.M. Chandrasekhar, J. Szczepanski, R.J. Van Zee, and W. Weltner Jr, J. Chem. Phys. **90**, 595 (1989); (b) P.F. Bernath, K.H. Hinkle, and J.J. Keady, Science **244**, 562 (1989); J. R. Health, A.L. Cooksy, M.H.W. Gruebele, C.A. Schmuttenmaer, and R.J. Saykally. Science **244**, 564 (1989); N. Moazzen-Ahmadi. A.R.W. McKeller, and T. Amano, J. Chem. Phys **91**, 2140 (1989); N. Moazzen-Ahmadi. A.R.W. McKeller, and T. Amano, J. Chem. Phys **157**, 1 (1989); (c) L.N. Shen and W.R.M. Graham, J. Chem. Phys. **91**, 5115; J.R. Health and R.J. Saykally, J. Chem. Phys. **94**, 3271 (1991).

[11] (a) D. Michalska, H. Chojnacki, B.A. Hess Jr, and L. Schaad, J. Chem. Phys. Lett. **141**, 376 (1987); (b) D.E. Bernholdt, D.H. Magers, and R.J. Bartlett, J. Chem. Phys. **89**, 3612 (1988); (c) J.M.L. Martin, J.P. Francois, and R. Gijbels, J. Chem. Phys. **90**, 3403 (1989).

[12] (a) J.M.L. Martin, J.P. Francois, and R. Gijbels, J. Chem. Phys. **93**, 8850 (1990); (b) J.M.L. Martin, J.P. Francois, and R. Gijbels, J. Comput. Chem. **12**, 52 (1991).

[13] M. Vala, T.M. Chandrasekhar, J. Szczepanski, and R. Pellow, in *Materials Chemistry at High Temperatures* edited by J. Hastie (Humana Press, Clifton, Nj, 1990) Vol. II; R.H. Kranze and W.R.M. Graham. J. Chem. Phys. **98** 71 (1993); H.J. Hwang, A. Vanorden, K. Tanaka, E.W. Kuo, J.R. Heath, and R.J. Saykally. J. Mol. Phys. **79**, 769 (1963); R.H. Kranze, P.A. Withey, C.M.L Rittby, and W.R.M. Graham, J. Chem. Phys. **105**, 5313 (1996).

[14] (a) J.R. Heath, R.A. Sheeks, A.L. Cooksy, and R.J. Saykally, Science **249**, 895 (1990); J.R. Health, A. Vanorden, E. Kuo, and R.J. Saykally, Chem. phys. Lett. **182**, 17 (1991); (b) J.R. Health and R.J Saykally, J. Chem. Phys. **94**, 1724 (1991); A. Vanorden, H.J. Hwang, E.W. Kuo, and R.J. Saykally, J. Chem. Phys. **98**, 6678 (1993).

[15] J.M.L. Martin, D.W. Schwenke, T.J. Lee, and P.R. Taylor, J. Chem. Phys. **104**, 4657 (1996) and references therein.

[16] S.J. Blanksby, D. Schröder, S. Dua, J.H. Bowie, and H. Schwarz, J. Am. Chem. Soc. **122**, 7105 (2000).

[17] J.M.L. Martin, J. El-Yazal, and J.-P. François, Chem. Phys. Lett. **242**, 570 (1995).

[18] J. Drowart, R.P. Burns, G. DeMaria, and M.G. Inghram, J. Chem. Phys. **31**, 1131 (1959).

[19] J.M.L. Martin, J.-P. François, and R. Gijbels, J. Chem. Phys. **95**, 9420 (1991).

[20] K.A. Gingerich, H.C. Finkbeiner, and R.W. Schmude Jr, J. Am. Chem. Soc. **116**, 3884 (1994).

[21] J.M.L. Martin and P.R. Taylor, J. Chem. Phys. **102**, 8270 (1995).

[22] A. Karton, E. Rabinovich, J.M.L. Martin, and B. Ruscic, J. Chem. Phys. **125**, 144108 (2006).

[23] (a) B. Ruscic, unpublished results obtained from Active Thermochemical Tables (ATcT) version 1.25 using the Core Argonne Thermochemical Network version 1.056 (2006); (b) B. Ruscic, R.E. Pinzon, M.L. Morton, N.K. Srinivasan, M.-C. Su, J.W. Sutherland, and

J.V. Michael, J. Phys. Chem. A **110**, 6592 (2006); (c) G. Tasi, R. Izsák, G. Matisz, A.G. Császár, M. Kállay, B. Ruscic, and J.F. Stanton, Chem. Phys. Chem. **7**, 1664 (2006); (d) B. Ruscic, R.E. Pinzon, M.L. Morton, G. von Laszewski, S. Bittner, S.G. Nijsure, K.A. Amin, M. Minkoff, and A.F. Wagner, J. Phys. Chem. A **108**, 9979 (2004); (e) B. Ruscic, *2005 Yearbook of Science and Technology* (annual update to *McGraw-Hill Encyclopedia of Science and Technology*) (McGraw-Hill, New York, 2004), pp. 3–7.

[24] C.X. Liang and H.F. Schaefer III, Chem. Phys. Lett. **169**, 150 (1990).

[25] C.X. Liang and H.F. Schaefer III, J. Chem. Phys. **93**, 8844 (1990).

[26] R.S. Grev, I.L. Alberts, and H.F. Schaefer III, J. Phys. Chem. A **94**, 3379 erratum **94**, 8744 (1990) (1990).

[27] M.L. Leininger, C.D. Sherrill, W.D. Allen, and H.F. Schaefer III, J. Chem. Phys. **108**, 6717 (1998).

[28] L. Belau, S.E. Wheeler, B.W. Ticknor, M. Ahmed, S.R. Leone, W.D. Allen, H.F. Schaefer III, and M.A. Duncan, J. Am. Chem. Soc. **129**, 10229 (2007).

[29] (a) K. Raghavachari, G.W. Trucks, J.A. Pople, and M. Head-Gordon, Chem. Phys. Lett. **157**, 479 (1989); (b) J.D. Watts, J. Gauss, and R.J. Bartlett, J. Chem. Phys. **98**, 8718 (1993).

[30] MOLPRO is a package of *ab initio* programs written by H.-J. Werner, P.J. Knowles, M. Schütz, R. Lindh, P. Celani, T. Korona, G. Rauhut, F.R. Manby, R.D. Amos, A. Bernhardsson, A. Berning, D.L. Cooper, M.J.O. Deegan, A.J. Dobbyn, F. Eckert, C. Hampel, G. Hetzer, A.W. Lloyd, S.J. McNicholas, W. Meyer, M.E. Mura, A. Nickla, P. Palmieri, R. Pitzer, U. Schumann, H. Stoll, A.J. Stone, R. Tarroni and T. Thorsteinsson. See also http://www.molpro.net.

[31] MRCC, a string-based general coupled cluster program suite written by M. Kállay. See also M. Kállay and P.R. Surján, J. Chem. Phys. **115**, 2945 (2001), http://www.mrcc.hu.

[32] ACES II (Mainz-Austin-Budapest version) is an electronic structure program system written by J.F. Stanton, J. Gauss, J.D. Watts, P.G. Szalay, and R.J. Bartlett, with contributions from A.A. Auer, D.E. Bernholdt, O. Christiansen, M.E. Harding, M. Heckert, O. Heun, C. Huber, D. Jonsson, J. Jusélius, W.J. Lauderdale, T. Metzroth, C. Michauk, D.P. O'Neill, D.R. Price, K. Ruud, F. Schiffmann, M.E. Varner, J. Vázquez and the integral packages MOLECULE (J. Almlöf and P.R. Taylor), PROPS (P.R. Taylor), and ABACUS (T. Helgaker, H.J. Aa. Jensen, P. Jørgensen, and J. Olsen). For the current version, see http://www.aces2.de.

[33] T.D. Crawford, C.D. Sherrill, E.F. Valeev, J.T. Fermann, R.A. King, M.L. Leininger, S.T. Brown, C.L. Janssen, E.T. Seidl, J.P. Kenny, and W.D. Allen, J. Comput. Chem. **28**, 1610 (2007), See also http://www.psicode.org.

[34] T.H. Dunning, J. Chem. Phys. **90**, 1007 (1989).

[35] K.A. Peterson and T.H. Dunning, J. Chem. Phys. **117**, 10548 (2002).

[36] W.A. de Jong, R.J. Harrison, and D.A. Dixon, J. Chem. Phys. **114**, 48 (2001).

[37] A. Karton and J.M.L. Martin, Theor. Chem. Acc. **115**, 330 (2006).

[38] F. Jensen, Theor. Chem. Acc. **113**, 267 (2005).

[39] W. Klopper, Mol. Phys. **99**, 481 (2001).

[40] A. Karton, P.R. Taylor, and J.M.L. Martin, J. Chem. Phys. **127**, 064104 (2007).

[41] J.M.L. Martin and G. de Oliveira, J. Chem. Phys. **111**, 1843 (1999); J.M.L. Martin and S. Parthiban, J. Chem. Phys. **114**, 6014 (2001).

[42] J.M.L. Martin and S. Parthiban, in *Quantum-Mechanical Prediction of Thermochemical Data. Understanding Chemical Reactivity*, edited by J. Cioslowski (Kluwer, Dordrecht, 2001), Vol. 22, Available online at: http://dx.doi.org/10.1007/0-306-47632-0_2.

[43] A.D. Boese, M. Oren, O. Atasoylu, J.M.L. Martin, M. Kállay, and J. Gauss, J. Chem. Phys. **120**, 4129 (2004).

[44] A. Karton, I. Kaminker and J.M.L. Martin, J. Phys. Chem. A, to be published.

[45] (a) M. Douglas and N.M. Kroll, Ann. Phys. (NY) **82**, 89 (1974); (b) B.A. Hess, Phys. Rev. A **33**, 3742 (1986).

[46] Gaussian 03, Revision C.01, M.J. Frisch, G.W. Trucks, H.B. Schlegel, G.E. Scuseria, M.A. Robb, J.R. Cheeseman, J.A. Montgomery, Jr., T. Vreven, K.N. Kudin, J.C. Burant, J.M. Millam, S.S. Iyengar, J. Tomasi, V. Barone, B. Mennucci, M. Cossi, G. Scalmani, N. Rega, G.A. Petersson, H. Nakatsuji, M. Hada, M. Ehara, K. Toyota, R. Fukuda, J. Hasegawa, M. Ishida, T. Nakajima, Y. Honda, O. Kitao, H. Nakai, M. Klene, X. Li, J.E. Knox, H.P. Hratchian, J.B. Cross, V. Bakken, C. Adamo, J. Jaramillo, R. Gomperts, R.E. Stratmann, O. Yazyev, A.J. Austin, R. Cammi, C. Pomelli, J.W. Ochterski, P.Y. Ayala, K. Morokuma, G.A. Voth, P. Salvador, J.J. Dannenberg, V.G. Zakrzewski, S. Dapprich, A.D. Daniels, M.C. Strain, O. Farkas, D.K. Malick, A.D. Rabuck, K. Raghavachari, J.B. Foresman, J.V. Ortiz, Q. Cui, A.G. Baboul, S. Clifford, J. Cioslowski, B.B. Stefanov, G. Liu, A. Liashenko, P. Piskorz, I. Komaromi, R.L. Martin, D.J. Fox, T. Keith, M.A. Al-Laham, C.Y. Peng, A. Nanayakkara, M. Challacombe, P.M.W. Gill, B. Johnson, W. Chen, M.W. Wong, C. Gonzalez and J.A. Pople (Gaussian, Inc., Wallingford, CT, 2004).

[47] T.J. Lee, J.E. Rice, G.E. Scuseria, and H.F. Schaefer III, Theor. Chim. Acta **75**, 81 (1989); T.J. Lee and P.R. Taylor ibid. **23**, 199 (1989).

[48] M.L. Leininger, I.M.B Nielsen, T.D. Crawford, and C.L. Janssen, Chem. Phys. Lett. **328**, 431 (2000); I.M.B Nielsen and C.L. Janssen, ibid. **310**, 658 (1999); C.L.Janssen and I.M.B. Nielsen, ibid. **290**, 423 (1998).

[49] C.D. Sherrill and P. Piecuch, J. Chem. Phys. **122**, 124104 (2005), and references therein.

[50] S.A. Kucharski, M. Kolaski, and R.J. Bartlett, J. Chem. Phys. **114**, 692 (2001).

[51] B. Ruscic, Private communication [unpublished data based on Active Thermochemical Tables, ATcT Version 1.25 and the Core (Argonne) Thermochemical Network Version 1.056 2006], quoted in D. Feller and K.A. Peterson, J. Chem. Phys, **126**, 114105 (2007).

[52] K.P. Huber and G. Herzberg, *Constants of Diatomic Molecules* (Van Nostrand Reinhold, New York, 1979).

[53] A. Karton and J.M.L. Martin, J. Chem. Phys. **120**, 144313 (2006).

[54] J.D. Watts and R.J. Bartlett, Chem. Phys. Lett. **190**, 19 (1992).

[55] V. Parasuk and J. Almlöf, Theor. Chim. Acta **83**, 227 (1992).

[56] Y. Shlyakhter, S. Sokolova, A. Lüchow, and J.B. Anderson, J. Chem. Phys. **110**, 10725 (1999).

[57] S. Grimme, J. Chem. Phys. **118**, 9095 (2003), For a physical interpretation of the SCS-MP2 method in terms of Feenberg scaling, see A. Szabados, J. Chem. Phys. **125**, 214105 (2006).

[58] T. Takatani, E.E. Hohenstein, and C.D. Sherrill, J. Chem. Phys. **128**, 124111 (2008), Those using quantum chemical codes such as MOLPRO that report E_S and E_T rather than $E_{\alpha\alpha}$, $E_{\beta\beta}$, and $E_{\alpha\beta}$ can easily obtain the SCS-CCSD correlation energy as $1.17666 E_T + 1.27 E_S$.

[59] L.A. Curtiss, K. Raghavachari, and J.A. Pople, J. Chem. Phys. **98**, 1293 (1993).

[60] L.A. Curtiss, K. Raghavachari, G.W. Trucks, and J.A. Pople, J. Chem. Phys. **94**, 7221 (1991).

[61] L.A. Curtiss, K. Raghavachari, P.C. Redfern, V. Rassolov, and J.A. Pople, J. Chem. Phys. **109**, 7764 (1998).

[62] A.G. Baboul, L.A. Curtiss, P.C. Redfern, and K. Raghavachari, J. Chem. Phys. **110**, 7650 (1999).

[63] L.A. Curtiss, P.C. Redfern, and K. Raghavachari, J. Chem. Phys. **126**, 084108 (2007).

[64] L.A. Curtiss, P.C. Redfern, and K. Raghavachari, J. Chem. Phys. **127**, 124105 (2007).

[65] J.A. Montgomery Jr, M.J. Frisch, J.W. Ochterski, and G.A. Petersson, J. Chem. Phys. **110**, 2822 (1999).

[66] J.W. Ochterski, G.A. Petersson, and J.A. Montgomery Jr, J. Chem. Phys. **104**, 2598 (1996).

[67] $C_2(^1\Sigma_g^+)$ W4.4 theory; $C_2(^3\Pi_u)$ W4.3 theory; C_3–C_5 W4 theory; $C_6(^3\Sigma_g^-)$ W4 theory via the $2C_4(^3\Sigma_g^-) \to C_6(^3\Sigma_g^-) + C_2(^3\Pi_u)$ reaction energy at the W3.2 level; $C_6(^1A_1')$ W3.2 theory; $C_7(^1\Sigma_g^+)$ W4 theory via the $2C_5(^1\Sigma_g^+) \to C_7(^1\Sigma_g^+) + C_3(^1\Sigma_g^+)$ reaction energy at the W3.2lite level; $C_8(^3\Sigma_g^-)$ W3.2 theory via the $2C_6(^3\Sigma_g^-) \to C_8(^3\Sigma_g^-) + C_4(^3\Sigma_g^-)$ reaction energy at the W3.2 level; $C_8(^1A_g)$ W3.2lite theory; $C_9(^1\Sigma_g^+)$ W4 theory via the $3C_5(^1\Sigma_g^+) \to C_9(^1\Sigma_g^+) + 2C_3(^1\Sigma_g^+)$ reaction energy at the W3.2 level; $C_{10}(^3\Sigma_g^-)$ W3.2lite theory via the $2C_6(^3\Sigma_g^-) \to C_{10}(^3\Sigma_g^-) + C_8(^3\Sigma_g^-)$ reaction energy at the W2.2 level; and $C_{10}(^1A_1')$ W2.2 theory.

[68] A.D. Boese and N.C. Handy, J. Chem. Phys. **114**, 5497 (2001).

[69] A.D. Becke, Phys. Rev. A **38**, 3098 (1988).

[70] C. Lee, W. Yang, and R.G. Parr, Phys. Rev. B **37**, 785 (1988).

[71] J.P. Perdew, J.A. Chevary, S.H. Vosko, K.A. Jackson, M.R. Pederson, D.J. Singh, and C. Fiolhais, Phys. Rev. B **46**, 6671 (1992).

[72] J.P. Perdew, Phys. Rev. B **33**, 8822 (1986).

[73] J.P. Perdew, K. Burke, and M. Ernzerhof, Phys. Rev. Lett. **77**, 3865 (1996) erratum **78**, 1396 (1997).

[74] Y. Zhao and D.G. Truhlar, J. Chem. Phys. **125**, 194101 (2006).

[75] T. van Voorhis and G.E. Scuseria, J. Chem. Phys. **109**, 400 (1998).

[76] J.M. Tao, J.P. Perdew, V.N. Staroverov, and G.E. Scuseria, Phys. Rev. Lett. **91**, 146401 (2003).

[77] A.D. Boese and N.C. Handy, J. Chem. Phys. **116**, 9559 (2002).

[78] C. Adamo and V. Barone, J. Chem. Phys. **110**, 6158 (1999).

[79] P.J. Wilson, T.J. Bradley, and D.J. Tozer, J. Chem. Phys. **115**, 9233 (2001).

[80] A.D. Becke, J. Chem. Phys. **98**, 5648 (1993).

[81] F.A. Hamprecht, A.J. Cohen, D.J. Tozer, and N.C. Handy, J. Chem. Phys. **109**, 6264 (1998).

[82] H.L. Schmider and A.D. Becke, J. Chem. Phys. **108**, 9624 (1998).

[83] V.N. Staroverov, G.E. Scuseria, J. Tao, and J.P. Perdew, J. Chem. Phys. **119**, 12129 (2003).

[84] P.J. Stephens, F.J. Devlin, C.F. Chabalowski, and M.J. Frisch, J. Phys. Chem. **98**, 11623 (1994).

[85] B.J. Lynch, P.L. Fast, M. Harris, and D.G. Truhlar, J. Phys. Chem. A **104**, 4811 (2000).

[86] C. Adamo and V. Barone, J. Chem. Phys. **108**, 664 (1998).

[87] A.D. Becke, J. Chem. Phys. **98**, 1372 (1993).

[88] Y. Zhao and D.G. Truhlar, J. Phys. Chem. A **108**, 6908 (2004).

[89] A.D. Becke, J. Chem. Phys. **104**, 1040 (1996).

[90] (a) Y. Zhao and D.G. Truhlar, Theor. Chem. Acc. **120**, 215 (2007); (b) Y. Zhao and D.G. Truhlar, Acc. Chem. Res. **41**, 157 (2008).

[91] Y. Zhao and D.G. Truhlar, J. Phys. Chem. A **109**, 5656 (2005).

[92] Y. Zhao, B.J. Lynch, and D.G. Truhlar, Phys. Chem. Chem. Phys. **7**, 43 (2005).

[93] Y. Zhao, N.E. Schultz, and D.G. Truhlar, J. Chem. Phys. **123**, 161103 (2005).

[94] A.D. Boese and J.M.L. Martin, J. Chem. Phys. **121**, 3405 (2004).

A. Karton et al.

[95] Y. Zhao, B.J. Lynch, and D.G. Truhlar, J. Phys. Chem. A **108**, 2715 (2004).

[96] S. Grimme, J. Chem. Phys. **124**, 034108 (2006).

[97] T. Schwabe and S. Grimme, Phys. Chem. Chem. Phys. **8**, 4398 (2006).

[98] A. Tarnopolsky, A. Karton, R. Sertchook, D. Vuzman, and J.M.L. Martin, J. Phys. Chem. A **112**, 3 (2008).

[99] A. Karton, A. Tarnopolsky, J.-F. Lamère, G.C. Schatz, and J.M.L. Martin, J. Phys. Chem. A **112**, 12868 (2008).

[100] F. Jensen, J. Chem. Phys. **115**, 9113 (2001) **116**, 3502(E) (2002).

[101] M.G. Giuffreda, M.S. Deleuze, and J.-P. François, J. Phys. Chem. A **106**, 8569 (2002).

[102] J.M.L. Martin, J. El-Yazal, and J.-P. François, Chem. Phys. Lett. **252**, 9 (1996).

[103] (a) G.A. Petersson, T. Tensfeldt, and J.A. Montgomery, J. Chem. Phys. **94**, 6091 (1991); (b) J.A. Montgomery, J.W. Ochterski, and G.A. Petersson, J. Chem. Phys. **101**, 5900 (1994); (c) G.A. Petersson (personal communication).